Ecology, 0(0), 2017, pp. 1–10

Phytoplankton size-scaling of net-energy flux across light and biomass gradients

Martino E. Malerba,[1] Craig R. White, and Dustin J. Marshall

Centre of Geometric Biology, School of Biological Sciences, Monash University, Melbourne, Victoria 3800 Australia

Abstract. Many studies examine how body size mediates energy use, but few investigate how size simultaneously regulates energy acquisition. Furthermore, rarely energy fluxes are examined while accounting for the role of biotic and abiotic factors in which they are nested. These limitations contribute to an incomplete understanding of how size affects the transfer of energy through individuals, populations, and communities. Here we characterized photosynthesis-irradiance (P-I) curves and per-cell net-energy use for 21 phytoplankton species spanning across four orders of magnitude of size and seven phyla, each measured across six light intensities and four population densities. We then used phylogenetic mixed models to quantify how body size influences the energy turnover rates of a species, and how this changes across environments. Rate-parameters for the P-I curve and net-energy budgets were mostly highly correlated and consistent with an allometric size-scaling exponent of <1. The energy flux of a cell decreased with population density and increased with light intensity, but the effect of body size remained constant across all combinations of treatment levels (i.e. no *size* × *population density* interaction). The negative effect of population density on photosynthesis and respiration is mostly consistent with an active downregulation of metabolic rates following a decrease in per-cell resource availability, possibly as an adaptive strategy to reduce the minimum requirements of a cell and improve its competitive ability. Also, because an increase in body size corresponds to a less-than-proportional increase in net-energy (i.e. exponent<1), we propose that volume-specific net-energy flux can represent an important cost of evolving larger body sizes in autotrophic single-cell organisms.

Key words: geometric biology; Kleiber's rule; light utilization; photosynthesis-irradiance (P-I) curve; phylogenetic mixed models; phytoplankton allometry; population density; respiration rates.

Introduction

Body size is perhaps the most definitive trait of a species. Size defines the rate at which organisms process energy and materials by imposing a suit of physical and chemical constraints on the individual (Calder 1984, Peters 1986). As such, most individual-level traits are correlated with size, such as growth (West et al. 2001), reproductive output (Enquist et al. 1999), and longevity (Marba et al. 2007). Thus, it is not surprising that many population-level processes also correlate with the size of the species. For instance, smaller species may show higher population densities (Damuth 1981, Peters and Wassenberg 1983, Enquist et al. 1998, Belgrano et al. 2002) and faster rates of population increase (Fenchel 1974, Blueweiss et al. 1978, Savage et al. 2004). These relationships determine the eco-evolutionary dynamics of a species and are also influential for broader community-level processes (Brown et al. 2004).

Almost a century ago, Huxley (1924), Kleiber (1932), and Brody et al. (1934) showed that many biological processes scale as power laws of the form:

$$R = a \times M^b \tag{1}$$

where R is some characteristics of an organism, such as the metabolic rate, M is the body size, a is the normalization constant, and b is the size-scaling exponent. Eq. 1 can be linearized as:

$$\ln R = \ln a + b \ln M. \tag{2}$$

There are now many estimates of metabolic size-scaling exponents across all levels of biological organisation, from individuals, to populations, to entire ecosystems (Belgrano et al. 2002, Brown et al. 2004). Despite many theories on the effects of size on energy utilization (metabolism), most empirical studies only focus on size and energy use, and largely ignore energy acquisition (Gillooly et al. 2001, Nagy 2005). For instance, estimates for size-scaling exponents of whole-individual metabolism vary widely with systematic variations among taxonomic groups (insects are >3/4, birds are <3/4, and protists are ~1), but overall they are mostly between 2/3 and 1 (West et al. 1997, 1999, Brown et al. 2004, Glazier 2006, 2009, Isaac and Carbone 2010). In contrast, less is known about the size-scaling of energy acquisition and considerable disparity exists between theoretical

Manuscript received 16 June 2017; revised 8 September 2017; accepted 18 September 2017. Corresponding Editor: Orlando Sarnelle.
[1] E-mail: Martino.Malerba@gmail.com

predictions and empirical data (Pawar et al. 2012, Rall et al. 2012). Clearly the overall effect of size on the energy budget of an organism will depend on how size affects both energy gain and use (together, net-energy gain). Yet, our understanding of size-dependent net-energy gain remains surprisingly poorly resolved.

The rate at which organisms use energy also depends on environmental conditions. For instance, predators often consume prey at a rate that depends not only on their size but also on a range of variables, such as prey availability (DeLong and Vasseur 2012, DeLong 2014), temperature (Englund et al. 2011, Rall et al. 2012), and density-dependent resource competition (DeLong and Hanson 2009*b*, a, Ghedini et al. in press). Ignoring environmental variables is likely to generate an incomplete understanding of the role of size, especially because many ecological rates (such as energy flux) change non-linearly across environmental gradients. In such cases, representing species using point-estimates will limit our ability to extrapolate beyond current conditions. An alternative approach to overcome this limitation is to focus on "function-valued traits" (sensu Stinchcombe et al. 2012), where parameters of (non-linear) functional responses are estimated across environmental gradients. Model parameters can be used to predict consumption rates for each species accounting for one or more variables. Function-valued approaches require more data, but offer greater comparability among studies, enhanced statistical power and flexibility, and can characterize the full range of environmental responses of a species (Stinchcombe and Kirkpatrick 2012). Thus, in recent years there has been an increase in popularity of studies using function-valued approaches (Savage et al. 2004, McGill et al. 2006, Violle et al. 2007, Stinchcombe et al. 2012, Goolsby 2015).

Photosynthesis is the engine that provides energy and organic matter for virtually all natural food webs on Earth. In particular, phytoplankton species are key primary producers, estimated to account for approximately half of the total carbon fixation on the planet (Field et al. 1998). Phytoplankton species range from 1 to 10^9 μm^3 in cell volume and represent an excellent example for the key importance of body size for the ecology and physiology of an organism (Maranon 2015). Size profoundly influences the performance of phytoplankton species across environmental gradients of light (Schwaderer et al. 2011, Edwards et al. 2015), nutrients (Litchman et al. 2007, Edwards et al. 2012, Maranon et al. 2013), and temperature (Thomas et al. 2012). While previous studies examined the role of size on either energy gain and/or energy use (Taguchi 1976, Blasco et al. 1982, Finkel et al. 2004, Lopez-Urrutia et al. 2006, Maranon 2008, Huete-Ortega et al. 2012, Lopez-Sandoval et al. 2014), few have investigated size-effects on the net-daily energy budget of a species, as the difference between net-photosynthesis during the day and respiration at night, integrated over the 24-h photoperiod. It seems obvious that the productivity of an organism will depend on how size simultaneously affects both energy gains and utilization – i.e., the net-energy flux. Also, the energy flux of a cell changes as a non-linear function of light availability, which depends not just on the external light source but also on the shading effect due to population density in solution (Huisman and Weissing 1994). Hence, a comprehensive analysis of the effects of size on daily net-energy flux requires characterizing multiple functions for how respiration and net-photosynthesis change across environmental gradients of light and population density.

The aim of this study is to investigate the effect of body size (measured as cell volume) on net energy flux of species across environmental conditions of light intensity and population density. To this end, we used 21 phytoplankton species from 7 phyla spanning 4 orders of magnitude in cell volume, all cultured and measured using identical protocols. Two replicate samples for each species were measured across a fully crossed experimental design of 6 light intensities (ranging from 0 to 250 at increments of 50 μm quanta m^{-2} s^{-1}) and 4 population densities (standardized by optical density), yielding a total of 24 light-density combinations for each of the 21 species. At each combination, energy rates were analyzed by fitting saturating photosynthesis-irradiance (P-I) curves.

Materials and Methods

Phytoplankton cultures and experimental design

Monoclonal batch cultures of the 21 species used in this experiment were sourced from the Australian National Algae Culture Collection (ANACC; see Fig. 1 for species names and strain codes) and reared in standard F/2 media, prepared with 0.45 μm filtered seawater (Guillard 1975). All species were cultured in aseptic 75 cm^2 plastic cell culture flasks (Corning®, Canted Neck, Nonpyrogenic) and grown in a temperature-controlled room at 21 ± 2°C with a 14–10 h day-night cycle with a light intensity of 150 μM m^{-2} s^{-1}. Species were handled aseptically with sterile materials under a laminar-flow cabinet (Gelman Sciences Australia, Model CF23S, National Association of Testing Authorities certified). Cell size was estimated by measuring at least 100 cells per species with optical light microscopy. Photos at 400× were taken of lugol-stained samples (2%) after loading 5 μL on a slide gently covered with a cover slip. Cell area was calculated with ImageJ and Fiji (version 2.0; Schindelin et al. 2012) and cell biovolume was calculated by assigning the most appropriate geometric shape for each species, as recommended by Sun and Liu (2003).

To evaluate any density-dependent effects, samples for each species were standardized across a gradient of population densities. The four levels of biomass concentrations were achieved by diluting mother cultures until reaching blank-corrected optical density values of 0.04

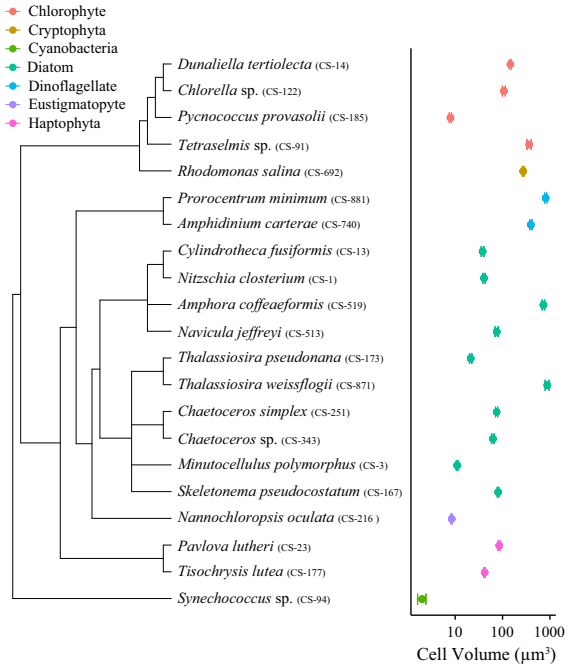

FIG. 1. Phylogeny of the species together with mean cell volume (±SE), strain code, and taxonomic group. All species were sourced from the Australian National Algae Culture Collection (ANACC) and the tree was compiled from the Tree of Life Web Project (Maddison et al. 2007; see material and methods for more details).

(10%), 0.12 (30%), 0.28 (70%), and 0.4 (100%), measured at 750 nm with microplate reader SPECTROstar® Nano (BMG labtech). Hence, each response variable was measured in a fully crossed factorial design of 21 species across 4 levels of population densities.

Dark and light metabolism

Methods for recording metabolic activity in the cultures were based on protocols by White et al. (2011) and Warkentin et al. (2007). Briefly, change in % oxygen saturation was monitored in 5 mL vials at 20°C using 24-channel PreSens sensor dish reader (SDR; AS-1 Scientific Wellington, New Zealand). Vials were fully filled, being careful to remove all air pockets. The rate of oxygen consumption of the whole sample ($\dot{V}O2$; units µmol O_2 min^{-1}) was measured as:

$$\dot{V}O2 = -1\frac{m_a - m_b}{100} V\beta O_2 \quad (3)$$

where m_a is the rate of change of O_2 saturation in each sample (min^{-1}), m_b is the mean O_2 saturation across all blanks of each plate (min^{-1}), V is the water volume (0.005 L), and βO_2 is the oxygen capacity of air-saturated seawater at 20°C and 35 ppt salinity (225 µmol O_2 L^{-1}). All sensors were calibrated with 0% and 100% air saturation before the experiment. Sodium bicarbonate (2 mM) was added to the media to ensure photosynthesis and oxygen evolution were not limited by carbon availability. All SDR were placed horizontally under the light source, to avoid cell deposition on top of the oxygen sensor at the base of the vial. Samples were randomly allocated to the top row of the SDR, while three blanks per reader were placed in the bottom rows. VO_2 measurements were taken at six light regimes (from 0 to 250 µM quanta m^{-2} s^{-1} at increments of 50), randomizing the order of light intensities and with dark periods separating each two light periods. Per-cell $\dot{V}O2$ ($\dot{V}O2_{cell}$; units µmol O_2 min^{-1} $cell^{-1}$) was calculated by dividing $\dot{V}O2$ by the total number of cells in the vial, measured by manual cell counting (Neubauer Improved hemocytometer, Bright-line double ruled, Pacific Lab).

Statistical analysis

Non-linear photosynthesis-irradiance (P-I) curves.— Photosynthesis-irradiance (P-I) curves of $\dot{V}O2_{cell}$ across 6 light intensities (E) were analysed by fitting curves by Platt et al. (1980) of the form:

$$\dot{V}O2_{cell,s,b} = P_{max,s,b}\left(1 - e^{-\left(\alpha_{s,b}\left(E - E_{c,s,b}\right)/P_{max,s,b}\right)}\right) \quad (4)$$

where s and b indicate the 21 species and the four biomass concentrations, respectively. $P_{max,s,b}$ is the maximum per-cell rate of oxygen production (units of µmol O_2 min^{-1} $cell^{-1}$), $\alpha_{s,b}$ is the initial slope of the curve (units of µmol O_2 min^{-1} $cell^{-1}$ (µmol quanta s^{-1} m^{-2})$^{-1}$), $E_{c,s,b}$ is the compensation photon flux (units µmol quanta s^{-1} m^{-2}). The mean respiration of a cell ($Resp_{s,b}$) is the Y-intercept of the curve (units of µmol O_2 min^{-1} $cell^{-1}$) and can be calculated as:

$$Resp_{s,b} = P_{max,s,b}\left(1 - e^{\alpha_{s,b} \times E_{c,s,b}/P_{max,s,b}}\right). \quad (5)$$

Alternative models of P-I curves (Eq. 4) including an inhibition term as an additional negative exponential function were also fitted, but likelihood ratio test between the two nested models showed little support for any light inhibition in the data. Non-linear P-I curves were calibrated using package nlme with the function nls in statistical software R (Pinheiro et al. 2016, R Core Team 2016). All models were visually inspected for goodness of fit and ensured to successfully converge.

Phylogenetic mixed models.—After fitting P-I curves to quantify the non-linear effect of light intensity on metabolic rates to 84 combinations of species (n = 21) and population density (n = 4), linear phylogenetic mixed models (Lynch 1991, Housworth et al. 2004) were used to analyse the effect of cell volume on each P-I parameter, on cell respiration, and on net-energy rates. We used the approach described by Kilmer and Rodriguez (2017) to calculate an attenuation factor (η) and correct for the

slope attenuation of having measurement error in cell volume, as follow: $\eta = var(X)/[var(X) + var(\varepsilon_X)]$, and $\bar{b} = \frac{b}{\eta}$, where $var(X)$ is the variance of cell volume across all species, $var(\varepsilon_X)$ is the variance around the mean cell volume of each species (the observation error), b is the size-scaling exponent without accounting for observation error around cell volume, and $\bar{b}$ is the size-scaling exponent adjusted for observation error on cell volume [hence $\bar{b} \approx b$, when $var(\varepsilon_X) \approx 0$]. We found that $\eta = 0.9914$, which means that measurement error of cell volume accounted for <1% of the total variance. We therefore divided all size-scaling exponents by 0.9914 to calculate size-scaling exponents adjusted for observation error on cell volume. Also, controlling for phylogenetic similarities in the data is necessary because traits of related species may be correlated and not statistically independent, especially for phytoplankton species (Connolly et al. 2008, Nakov et al. 2014). This dependency violates the assumption of most statistical tests and need to be incorporated in the variance structure. Therefore, univariate phylogenetic mixed models were implemented following Hadfield (2010) to analyze the effects of cell size, population density, and their interaction on metabolic rates. If credible intervals for the interaction coefficient overlapped 0, models were re-fitted including only main effects.

We analyzed the oxygen evolution of a cell (units μmol O_2 h^{-1} $cell^{-1}$) by fitting phylogenetic mixed models to each of the P-I parameters (i.e. P_{max}, E_c, and α). The uncertainty associated with fitting non-linear P-I curves to observations (Eq. 4) was included by associating measurement error variance to each estimated P-I parameter. Then, we analyzed the energy use of a cell by fitting phylogenetic mixed models to per-cell daily net-energy production and per-cell daily respiration. Both energy rates were calculated by transforming the units of the P-I parameters from oxygen evolution (μmol O_2 d^{-1} $cell^{-1}$) to calorific energy (Joules d^{-1} $cell^{-1}$) using the conversion of 512×10^{-3} J $(\mu mol\ O_2)^{-1}$ from Williams and Laurens (2010), which assumes a cell macromolecular composition of 35% protein, 35% carbohydrates, 25% lipids, and 5% nucleic acid. P-I curves (Eq. 4) with energy-converted parameters where then used to calculate per-cell daily net-energy production (units Joules d^{-1} $cell^{-1}$) as the difference between net-photosynthesis during the day and respiration at night, assuming 16:8 photoperiod and light intensities of either 50, 100, 150, 200, and 250 μmol quanta m^{-2} s^{-1}. Similarly, per-cell daily respiration rates (units Joules d^{-1} $cell^{-1}$) were calculated assuming 24 h of darkness.

The phylogeny of the species was included in the variance structure of the model as a random effect and was compiled from the Tree of Life Web Project (Maddison et al. 2007) using the R packages rotl (Michonneau et al. 2016) and MCMCglmm (Hadfield 2010). The length of each branch is proportional to the taxonomic relatedness from the node where the branch leads. Phylogenetic heritability is the proportion of variance associated with the random effect of the phylogeny (between 0 and 1) and is equivalent to the parameter λ (Hadfield and Nakagawa 2010), which is commonly used as a metric of the degree of phylogenetic correlation in the data (Pagel 1999, Freckleton et al. 2002). When λ = 0, traits are phylogenetically independent, while when λ = 1 traits are phylogenetically correlated as expected when assuming evolution to follow Brownian motion. However, the tree used here also suffers from two nodes that have not been fully resolved (polytomy; Fig. 1). This is probably due to their close relationship and the limitations on diatom taxonomy. To confirm our results, we repeated the analysis by replacing the phylogenetic variance structure with taxonomic-independent species-specific random effects and confirmed that this did not change any of the conclusions. Finally, because there are multiple observations for species, a second species-specific random effect was initially included in our full model. However, model selection with deviance information criterion (Hooten and Hobbs 2015) selected against this second random effect and it was therefore removed from the final model.

Every dataset was sampled 1.3×10^6 times with Metropolis-Hastings sampler, following 3×10^5 iterations for burn-in, and a thinning of 1000, using software R with package MCMCglmm (Hadfield 2010, R Core Team 2016). All priors for the parameters were uninformative from an inverse Wishard distribution. To monitor successful convergence, we inspected the iterated history, density plot, and ensured Geweke z-score between −2 and 2 (Geweke 1992). Packages coda ggplot2 (Wickham 2009), (Plummer et al. 2006), ggmcmc (Marín 2015), and PerformanceAnalytics (Peterson and Carl 2014) were also used for statistical analyses and plots. Mean and credible intervals were calculated from the posterior distributions of each parameter.

Partial residuals were used to calculate the unique contribution of cell size on metabolic rates while controlling for the effects of population density, as:

$$\left(Y_{Obs,i} - Y_{Pred,i}\right) + \beta \times size_i + \alpha + \partial \times conc \qquad (6)$$

where α and β are the intercept and slope of size, $size_i$ is the cell volume of ith observation, ∂ is the coefficient for population density, $conc$ is the mean value of population density in the data, and $Y_{Obs,i}$ and $Y_{Pred,i}$ are the observed metabolic rates and the metabolic rates predicted by the phylogenetic mixed model, respectively. Analogous calculations were made to determine the effects of population density while controlling for size (i.e. replace $size_i$ with $size$ and $conc$ with $conc_i$).

Results

P-I parameters

Cell volume explained a large proportion of the variation in P-I curve parameters among species (Fig. 2; Table 1). Maximum photosynthetic rate (P_{max}) and initial slope of the P-I curve (*alpha*) were highly positively

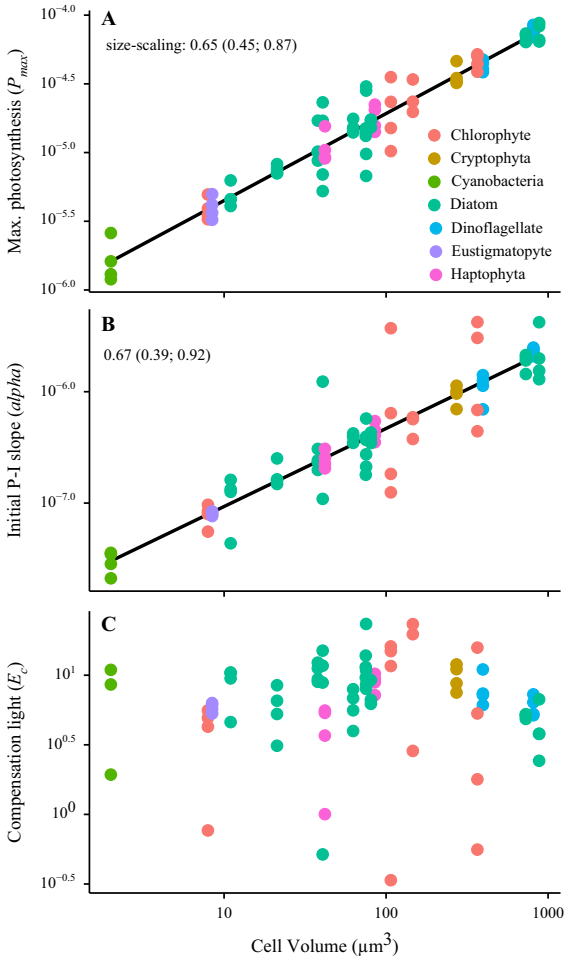

FIG. 2. Allometric relationships and size-scaling exponents (±95% credible intervals) for the three parameters of the P-I curve. Plotted observations are corrected for the effect of population density, by plotting partial residuals for cell volume (see Eq. 6). P_{max} is the maximum per-cell rate of oxygen production (units of µmol O_2 h^{-1} $cell^{-1}$), α is the initial slope of the P-I curve (µmol O_2 h^{-1} $cell^{-1}$ (µmol quanta s^{-1} m^{-2})$^{-1}$), and E_c is the compensation photon flux (units µmol quanta s^{-1} m^{-2}).

correlated (Appendix S1: Fig. S1) and scaled allometrically with cell size at an exponent of <1 (Fig. 2A, B; Table 1). Furthermore, the light level at which respiration perfectly balanced photosynthesis (*Ec*) was independent to either P_{max} or *alpha* (Appendix S1: Fig. S1) and showed no relationship with cell size and population density (Fig. 2C; Table 1). All interaction terms between cell size and population density overlapped 0 for all P-I parameters and were therefore removed from the final model (Table 1).

Daily net-energy production and respiration

Daily rates for per-cell net-energy production and respiration scaled allometrically with size at an exponent consistently <1 (Fig. 3A, C; Table 1). This indicates that increasing body size corresponded to a less-than-proportional increase in net-energy production and respiration of a cell. Specifically, for a 3 orders of magnitude increase in cell volume, rates of net-energy production and respiration only increased by 1.9 and 2.1 orders of magnitude, respectively.

Decreasing population density increased the energy produced by a cell and its respiration rate (Fig. 3B, D), while net-energy production also increased with higher light exposure (Fig. 3A). On average, diluting population density 10 times (optical density from 0.4 to 0.04) recorded 2.2 times higher per-cell net-energy production (Fig. 3B) and 2.3 times higher per-cell respiration (Fig. 3D). Similarly, cells increased their net-energy production by 2.1 times when increasing light intensity from 50 µm quanta m^{-2} s^{-1} to 250 µm quanta m^{-2} s^{-1} (Fig. 3A, after converting to arithmetic scale).

Increasing the size of a cell or decreasing population density produced similar proportional increases in both rates of energy production and respiration (notice parallel lines and similar slope coefficients between Fig. 3A, C and between Fig. 3B, D). This explains why the breakeven light intensity where respiration equals photosynthesis (parameter *Ec*) was not affected by either cell size or population density (Table 1): since per-cell net-energy production was positively correlated to per-cell respiration (r = 0.84), their difference would tend to remain constant across all levels of cell size and population density (Table 1). Finally, all interaction terms between cell size and population density overlapped 0 for all rates of net-energy production and respiration: this implies that the effect of size was constant across all levels of population densities (Fig. 3; Table 1).

DISCUSSION

Almost every parameter describing photosynthesis, respiration, and net-energy flux of a cell scaled allometrically with exponents of <1 with cell size. The only exception was compensation light intensity (i.e. the breakeven light intensity where respiration equals photosynthesis, or net-photosynthesis equals 0: E_c), indicating that the minimum amount of light required to maintain cell energy is similar across a 3 orders of magnitude size range. This is because larger cells produced more energy but also had higher energy costs due to respiration. Furthermore, increasing population density or decreasing light irradiance systematically reduced photosynthesis, respiration, and the net-energy production of a cell (i.e., different intercepts), but did not alter any of the size-scaling exponents (i.e., same slopes among allometric lines).

Empirical studies across all major phytoplankton phyla showed that per-cell rates of nutrient assimilation mostly scale isometrically with cell volume, while the minimum nutrient requirement for growth scales allometrically at an exponent of <1 (Maranon et al. 2013, Maranon 2015). Combining these two size-scaling exponents yields the prediction that volume-standardized nutrient uptake does not change with size and that larger

TABLE 1. Mean estimates and credible intervals for fixed effects and phylogenetic heritability coefficients (λ) of all mixed models for P-I curve parameters and for per-cell daily net-energy flux (J d^{-1} $cell^{-1}$). P-I parameters are maximum per-cell rate of oxygen production (P_{max}), initial slope of the curve (α), and compensation photon flux (E_c; see Fig. 2 for parameter units). Per-cell respiration is calculated assuming 24 h of darkness [transformed in the model as $\log_e$ (– per-cell respiration)]. Rates of per-cell net energy production are calculated as the difference between respiration and photosynthesis assuming 16:8 photoperiod and light intensities (L) of either 50, 100, 150, 200, or 250 μmol quanta m^{-2} s^{-1}. All size-scaling coefficients were adjusted for the effect of observation error on cell size using an attenuation factor (η) of 0.9914 (see *Phylogenetic mixed models* in *Materials and Methods* section). All interaction terms between $\log_{10}$(cell volume) and Pop. density were overlapping 0 and were therefore removed from the final model (see *Phylogenetic models* in *Materials and Methods* section).

	Intercept	$\log_{10}$(cell volume)	Pop. density	Phylo. heritability (λ)
P-I parameters				
$\log_e$ (*Pmax*)	−13.17 (−14.93; −11.27)	0.65 (0.45; 0.87)	−0.008 (−0.010; −0.006)	0.960 (0.91; 0.98)
$\log_e$ (*alpha*)	−16.95 (−19.34; −14.35)	0.67 (0.39; 0.92)	−0.012 (−0.015; −0.010)	0.940 (0.87; 0.98)
Ec	1.33 (−1.06; 3.11)	0.05 (−0.37; 0.47)	0.008 (−0.017; 0.031)	0.190 (0.003; 0.55)
Daily per-cell net-energy				
$\log_e$ (Resp.)	−12.39 (−14.69; −9.87)	0.73 (0.43; 0.99)	−0.009 (−0.013; −0.005)	0.912 (0.82; 0.96)
$\log_e$ (L = 50)	−11.83 (−14.28; −9.69)	0.65 (0.37; 0.93)	−0.012 (−0.014; −0.008)	0.953 (0.9; 0.98)
$\log_e$ (L = 100)	−11.53 (−13.95; −9.13)	0.64 (0.39; 0.91)	−0.009 (−0.011; −0.006)	0.966 (0.93; 0.99)
$\log_e$ (L = 150)	−11.32 (−13.41; −9.07)	0.64 (0.42; 0.88)	−0.008 (−0.010; −0.005)	0.952 (0.91; 0.98)
$\log_e$ (L = 200)	−11.24 (−13.21; −9.34)	0.63 (0.41; 0.85)	−0.007 (−0.010 −0.005)	0.940 (0.87; 0.98)
$\log_e$ (L = 250)	−11.29 (−13.31; −9.41)	0.64 (0.39; 0.84)	−0.007 (−0.010; −0.004)	0.930 (0.85; 0.97)

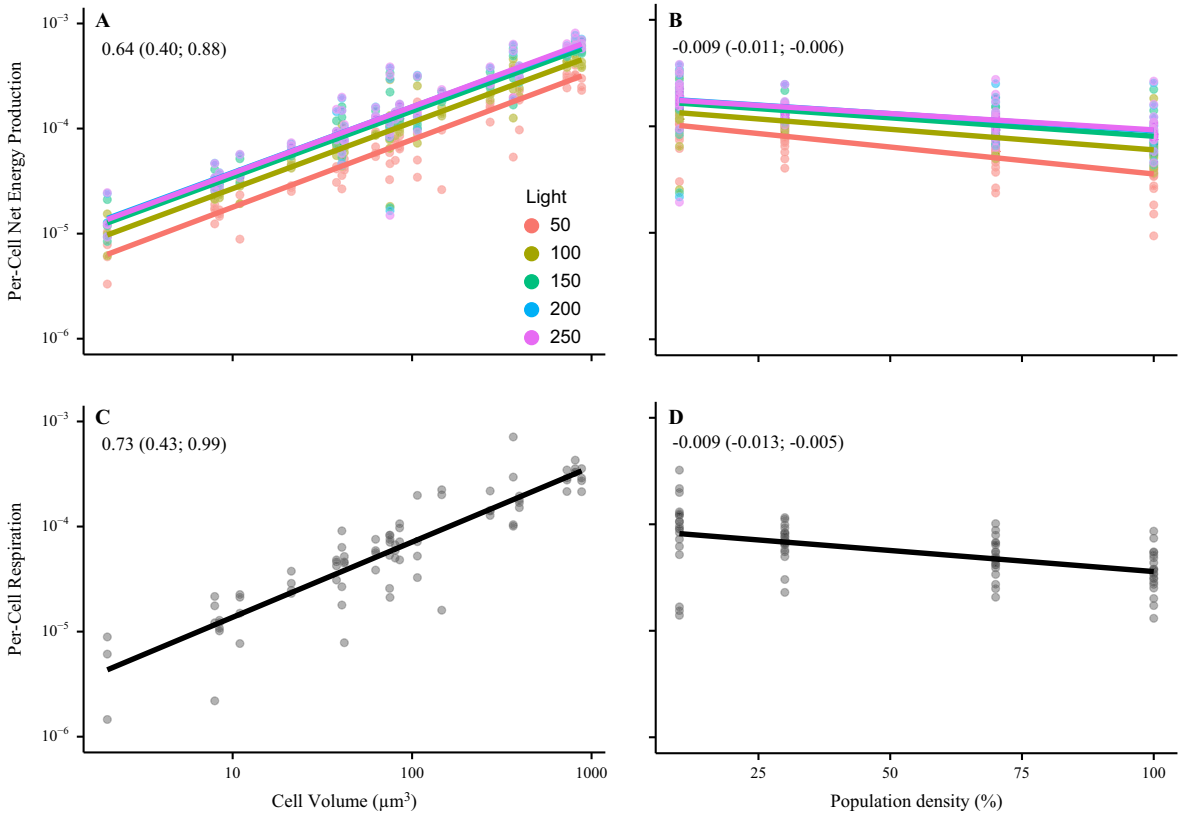

FIG. 3. Effect of cell volume and (B, D) population density on per-cell net energy flux (A, B) and per-cell respiration (C, D; units J d^{-1} $cell^{-1}$). Daily rates were calculated by assuming 16:8 photoperiod (see *Phylogenetic mixed models* section in *Material and Methods*), with net-energy flux calculated as a function of light intensity, from 50 to 250 μmol quanta m^{-2} s^{-1}. Rates of energy use during dark respiration are all <0; in order to allow log-transformation in the model, per-cell respiration rates are calculated as $\log_{10}$(–per-cell energy use). All relationships were corrected for the effects of other explanatory variables in the model by computing model partial residuals (see Eq. 6). Mean coefficients (± 95% credible intervals) for the effects of cell volume and population density are also shown (see Table 1). Population densities in the experiment were standardized among species using optical density values of 0.04, 0.12, 0.28 and 0.4, here represented as percentages of 10%, 30%, 70%, and 100%, respectively. See Table 1 for model coefficients.

cells require less nutrients per unit volume. Thus, increasing cell size should allow the assimilation of nutrients at rates far greater than their minimum requirements and can therefore represent an evolutionary advantage. However, our results and those from others Finkel et al. (2004) indicate that phytoplankton net-photosynthesis scales at an exponent of <1, such that increasing cell volume leads to a less-than-proportional rate at which energy can be produced and utilized. Hence, while species with larger cells are advantaged by obtaining more nutrients than required, they are also limited by their volume-specific rates of net energy production. This may explain why smaller unicellular species often show faster maximum population growth rates than larger species (Savage et al. 2004, but see also Maranon 2015 for unimodal size-scaling of growth rate). The ability of a species to store energy can also mediate the role of cell size on the fitness of a species (Grover 1991, 2011). Lipids and carbohydrates are the main sources of energy storage in phytoplankton: Carbohydrates are accumulated as starch-like granules and are more energy efficient, but also take up more intracellular space than lipids (up to 20% of cellular space in small cell species; Finkel et al. 2016). While there is considerable variability on the size-scaling exponent of stored energy among taxonomic groups (Hitchcock 1982, Moal et al. 1987, Finkel et al. 2016), reduced intracellular space of smaller cells may limit the amount of stored carbohydrates and affect their ability to endure periods of darkness or low resource regimes.

Here we found a negative effect of population density on per-capita rates of photosynthesis and respiration. This finding is in agreement with several other studies showing a reduction in metabolic rate in response to increasing population density for both autotrophic and heterotrophic species (phytoplankton: DeLong and Hanson 2009*a,b*, other invertebrates: DeLong 2014, Ghedini et al. in press, fish: Nadler et al. 2016). While previous studies involved isolated species, we now show that such negative effect equally applies across a taxonomically diverse community of 21 species. Moreover, our results indicate that the strength of this negative effect is proportional across species of widely different body sizes. Specifically, increasing population density 10 times (from 10% to 100%) decreased per-capita net energy flux and respiration by about half an order of magnitude. Increasing population density also decreases the quality and quantity of available photosynthetically-active radiation (between 400 and 700 nm), as light is transmitted through suspended phytoplankton cells (Holmes and Smith 1977), potentially explaining this photosynthetic downregulation. However, this does not explain why population density also decreases respiration rates in the dark. Especially because we found no relationship between the respiration rate of a cell and its previously experienced light intensity ($F_{1,818} = 1.53$, $P = 0.2$). Instead, the effects of population density are mostly consistent with an active downregulation of metabolic rates following a decrease in per-capita resources. DeLong and Hanson (2009*a*) previously found density-dependent regulation of metabolic rate in four unicellular organisms. It is therefore possible that reducing metabolic rates at increasing population densities can represent an adaptive strategy to reduce the minimum requirements of a cell and improve its fitness when competing for limiting resources.

Theoretical models describing the bio-optical properties of autotrophic cells predict a decrease in size-scaling exponent with decreasing light intensities, as larger cells can be more affected by low light conditions than smaller cells, due to higher "package effect" (i.e. intracellular self-shading reducing the capacity of pigments to harvest light; Finkel and Irwin 2000, Finkel et al. 2004, Mei et al. 2009). Instead, our results failed to detect any differences in the size-scaling exponents across light intensities between 50 and 250 μmol photon m^{-2} s^{-1} (i.e. only intercepts differed across environmental conditions). However, notice that most previous studies on the effects of light intensity on size-scaling exponents focused exclusively on photosynthetic rates, without also including the contribution of respiration rates on the net-photosynthesis of a cell. The dominant source of respiration in most autotrophic organisms is proportional to their growth and photosynthetic rates [due to oxygen-consuming and energy-dissipating pathways such as photorespiration and Mehler reaction (Langdon 1993, Lewitus and Kana 1995, Williams and Laurens 2010)]. If self-shading leads to reductions in both photosynthesis and respiration, we would expect some degree of compensation in net-photosynthetic rates and also in the variability of size-scaling exponents across light intensities.

Size-scaling exponents for photosynthesis and respiration are usually calculated by representing each species as point-estimates, standardized as either measured in the dark or after ensuring optimal light regimes for each species (e.g. Maranon et al. 2007, Lopez-Sandoval et al. 2014). Our alternative approach of estimating size-scaling exponents after fitting P-I curves was motivated by concerns that traditional point-estimates might provide poor understanding of non-linear relationships between energy rates and light and biomass levels (Kingsolver et al. 2001, 2014, Stinchcombe et al. 2012). Yet ironically, our study indicates that calculating size-scaling exponents by measuring each species only once can provide equally reliable size-scaling exponents in the most time- and resource-efficient way. This is because we found that rates of energy production and respiration were highly correlated and they all produced very similar size-scaling coefficients.

The size-scaling exponents for primary production and respiration documented here are in agreement with studies by Finkel et al. (2004), Lopez-Urrutia et al. (2006), Gillooly et al. (2001), and Brown et al. (2004). However, they also contradict a number of recent studies reporting isometric scaling exponents for phytoplankton metabolic rates, both in the field (Maranon et al. 2007, Huete-Ortega et al. 2012) and in the laboratory (Lopez-Sandoval

et al. 2014). Differences in statistical techniques could partly explain these conflicting results: exponents close to 1 were calculated using Reduced Major Axis (RMA) techniques. Slopes calculated with RMA have higher exponents than traditional ordinary least squares (OLS), as $slope_{RMA} = slope_{OLS}/\sqrt{r^2}$ with r as the correlation coefficient. Thus, $slope_{RMA}$ approaches ∞ as r approaches 0 (Griffiths 1998). Furthermore, given that cell mass scales allometrically at <1 with cell volume in phytoplankton species (Menden-Deuer and Lessard 2000), size-scaling exponents based on mass will be higher than those based on volume. Here cell size was measured as volume, whereas most previous phytoplankton allometric studies used cell mass. Another explanation could be that previous studies measured photosynthetic rates as carbon fixation using radiolabelling and ^{14}C isotopes, while we used bio-optical methods to track oxygen evolution. Both methods have limitations: the former is less sensitive to small oxygen changes, while the latter cannot account for remineralization and depends on laboratory protocols (e.g. incubation time). Estimates of primary productivity among methods remain poorly comparable (reviewed in Regaudie-de-Gioux et al. 2014). Finally, the discrepancy between our studies and previous analyses could also be due to the incorporation of phylogenetic information in our analysis. Previous studies did not correct for taxonomic correlation and this will overestimate degrees of freedom and increase type I error in the analyses. However, the tree used here suffers from two unresolved nodes, which will need to be resolved to fully confirm all taxonomic correlations among species.

The present study showed that increasing body size lead to a reduction in the volume-specific net-energy flux of autotrophic unicellular species, potentially representing an additional evolutionary cost of increasing cell size. This is consistent with small species often dominating in low-light environments. However, phytoplankton species range over nine orders of magnitude in cell volume, which means that evolving larger cells must have other non-energetic evolutionary benefits (e.g. lower grazing susceptibility, higher ability to store nutrients). Moreover, we showed that the energy flux of a cell decreased with population density, as both net-photosynthesis and respiration are downregulated as per-capita resources decrease. As already proposed by DeLong and Hanson (2009*a*), we also believe that density-dependent metabolism could represent an important and widespread strategy to minimize energy requirement and improve the ability of an individual to compete for resources. Finally, it is increasingly apparent that global temperature increases are reducing body sizes worldwide, particularly of aquatic organisms (Daufresne et al. 2009, Forster et al. 2012, Peter and Sommer 2012). While the mechanisms driving this decrease in body size are poorly understood, it is likely to involve the higher volume-specific energy production of smaller organisms. If this is the case, we would predict that future phytoplankton communities should display higher mass-specific net-energy flux and potentially improve current rates of ocean carbon sequestration.

Acknowledgments

We thank handling editor and anonymous reviewers for their insightful comments. We also thank Dr Maria del Mar Palacios Otero, Lucy Chapman, Belinda Comerford, Annie Guillaume, and staff at the Australian National Algae Culture Collection (ANACC) for their help with laboratory procedures. We also thank the Australian Research Council for financial support. The authors declare no conflict of interest.

Literature Cited

Belgrano, A., A. P. Allen, B. J. Enquist, and J. F. Gillooly. 2002. Allometric scaling of maximum population density: a common rule for marine phytoplankton and terrestrial plants. Ecology Letters 5:611–613.

Blasco, D., T. T. Packard, and P. C. Garfield. 1982. Size dependence of growth-rate, respiratory electron-transport system activity, and chemical-composition in marine diatoms in the laboratory. Journal of Phycology 18:58–63.

Blueweiss, L., H. Fox, V. Kudzma, D. Nakashima, R. Peters, and S. Sams. 1978. Relationships between body size and some life history parameters. Oecologia 37:257–272.

Brody, S., R. C. Procter, and U. S. Ashworth. 1934. Basal metabolism, endogenous nitrogen, creatinine and neutral sulphur excretions as functions of body weight. University of Missouri Agricultural Experiment Station Research Bulletin 220:1–40.

Brown, J. H., J. F. Gillooly, A. P. Allen, V. M. Savage, and G. B. West. 2004. Toward a metabolic theory of ecology. Ecology 85:1771–1781.

Calder, W. A. 1984. Size, function, and life history. Courier Corporation.

Connolly, J. A., M. J. Oliver, J. M. Beaulieu, C. A. Knight, L. Tomanek, and M. A. Moline. 2008. Correlated evolution of genome size and cell volume in diatoms (Bacillariophyceae)(1). Journal of Phycology 44:124–131.

Damuth, J. 1981. Population density and body size in mammals. Nature 290:699–700.

Daufresne, M., K. Lengfellner, and U. Sommer. 2009. Global warming benefits the small in aquatic ecosystems. Proceedings of the National Academy of Sciences of the United States of America 106:12788–12793.

DeLong, J. P. 2014. The body-size dependence of mutual interference. Biology Letters 10:20140261.

DeLong, J. P., and D. T. Hanson. 2009*a*. Density-dependent individual and population-level metabolic rates in a suite of single-celled eukaryotes. The Open Biology Journal 2:32–37.

DeLong, J. P., and D. T. Hanson. 2009*b*. Metabolic rate links density to demography in *Tetrahymena pyriformis*. ISME Journal 3:1396–1401.

DeLong, J. P., and D. A. Vasseur. 2012. Size-density scaling in protists and the links between consumer–resource interaction parameters. Journal of Animal Ecology 81:1193–1201.

Edwards, K. F., M. K. Thomas, C. A. Klausmeier, and E. Litchman. 2012. Allometric scaling and taxonomic variation in nutrient utilization traits and maximum growth rate of phytoplankton. Limnology and Oceanography 57:554–566.

Edwards, K. F., M. K. Thomas, C. A. Klausmeier, and E. Litchman. 2015. Light and growth in marine phytoplankton: allometric, taxonomic, and environmental variation. Limnology and Oceanography 60:540–552.

Englund, G., G. Öhlund, C. L. Hein, and S. Diehl. 2011. Temperature dependence of the functional response. Ecology Letters 14:914–921.

Enquist, B. J., J. H. Brown, and G. B. West. 1998. Allometric scaling of plant energetics and population density. Nature 395:163–165.

Enquist, B. J., G. B. West, E. L. Charnov, and J. H. Brown. 1999. Allometric scaling of production and life-history variation in vascular plants. Nature 401:907–911.

Fenchel, T. 1974. Intrinsic rate of natural increase: the relationship with body size. Oecologia 14:317–326.

Field, C. B., M. J. Behrenfeld, J. T. Randerson, and P. Falkowski. 1998. Primary production of the biosphere: integrating terrestrial and oceanic components. Science 281:237–240.

Finkel, Z. V., and A. J. Irwin. 2000. Modeling size-dependent photosynthesis: light absorption and the allometric rule. Journal of Theoretical Biology 204:361–369.

Finkel, Z. V., A. J. Irwin, and O. Schofield. 2004. Resource limitation alters the 3/4 size scaling of metabolic rates in phytoplankton. Marine Ecology Progress Series 273:269–279.

Finkel, Z., M. Follows, and A. Irwin. 2016. Size-scaling of macromolecules and chemical energy content in the eukaryotic microalgae. Journal of Plankton Research 38:1151–1162.

Forster, J., A. G. Hirst, and D. Atkinson. 2012. Warming-induced reductions in body size are greater in aquatic than terrestrial species. Proceedings of the National Academy of Sciences of the United States of America 109:19310–19314.

Freckleton, R. P., P. H. Harvey, and M. Pagel. 2002. Phylogenetic analysis and comparative data: a test and review of evidence. American Naturalist 160:712–726.

Geweke, J. F. 1992. Evaluating the accuracy of sampling-based approaches to the calculation of posterior moments. Pages 169–193 *in* J. O. Berger, J. M. Bernardo, A. P. Dawid and A. F. M. Smith, editors. Bayesian statistics 4. Clarendon Press, Oxford, UK.

Ghedini, G., C. R. White, and D. J. Marshall. *in press.* Does energy flux predict density-dependence? An empirical field test. Ecology doi/10.1002/ecy.2033/full.

Gillooly, J. F., J. H. Brown, G. B. West, V. M. Savage, and E. L. Charnov. 2001. Effects of size and temperature on metabolic rate. Science 293:2248–2251.

Glazier, D. S. 2006. The 3/4-power law is not universal: evolution of isometric, ontogenetic metabolic scaling in pelagic animals. AIBS Bulletin 56:325–332.

Glazier, D. S. 2009. Metabolic level and size scaling of rates of respiration and growth in unicellular organisms. Functional Ecology 23:963–968.

Goolsby, E. W. 2015. Phylogenetic comparative methods for evaluating the evolutionary history of function-valued traits. Systematic Biology 64:568–578.

Griffiths, D. 1998. Sampling effort, regression method, and the shape and slope of size-abundance relations. Journal of Animal Ecology 67:795–804.

Grover, J. P. 1991. Resource competition in a variable environment: phytoplankton growing according to the variable-internal-stores model. American Naturalist 138:811–835.

Grover, J. P. 2011. Resource storage and competition with spatial and temporal variation in resource availability. American Naturalist 178:E124–E148.

Guillard, R. R. L. 1975. Culture of phytoplankton for feeding marine invertebrates. Pages 26–60 *in* W. L. Smith and M. H. Chanley, editors. Culture of marine invertebrate animals. Plenum Press, New York, USA.

Hadfield, J. D. 2010. MCMC methods for multi-response generalized linear mixed models: the MCMCglmm R package. Journal of Statistical Software 33:1–22.

Hadfield, J. D., and S. Nakagawa. 2010. General quantitative genetic methods for comparative biology: phylogenies, taxonomies and multi-trait models for continuous and categorical characters. Journal of Evolutionary Biology 23:494–508.

Hitchcock, G. L. 1982. A comparative study of the size-dependent organic composition of marine diatoms and dinoflagellates. Journal of Plankton Research 4:363–377.

Holmes, M. G., and H. Smith. 1977. The function of phytochrome in the natural environment. II. The influence of vegetation canopies on the spectral energy distribution of natural daylight. Photochemistry and Photobiology 25:539–545.

Hooten, M. B., and N. T. Hobbs. 2015. A guide to Bayesian model selection for ecologists. Ecological Monographs 85:3–28.

Housworth, E. A., E. P. Martins, and M. Lynch. 2004. The phylogenetic mixed model. American Naturalist 163:84–96.

Huete-Ortega, M., P. Cermeno, A. Calvo-Diaz, and E. Maranon. 2012. Isometric size-scaling of metabolic rate and the size abundance distribution of phytoplankton. Proceedings. Biological Sciences 279:1815–1823.

Huisman, J., and F. J. Weissing. 1994. Light-limited growth and competition for light in well-mixed aquatic environments - an elementary model. Ecology 75:507–520.

Huxley, J. S. 1924. Constant differential growth-ratios and their significance. Nature 114:895.

Isaac, N. J., and C. Carbone. 2010. Why are metabolic scaling exponents so controversial? Quantifying variance and testing hypotheses. Ecology Letters 13:728–735.

Kilmer, J. T., and R. L. Rodriguez. 2017. Ordinary least squares regression is indicated for studies of allometry. Journal of Evolutionary Biology 30:4–12.

Kingsolver, J. G., R. Gomulkiewicz, and P. A. Carter. 2001. Variation, selection and evolution of function-valued traits. Genetica 112–113:87–104.

Kingsolver, J., S. Diamond, and R. Gomulkiewicz. 2014. Curve-thinking: understanding reaction norms and developmental trajectories as traits. Pages 39–53 *in* L. B. Martin, C. K. Ghalambor, and H. A. Woods, editors. Integrative Organismal Biology. John Wiley & Sons, Inc, Hoboken, New Jersey, USA.

Kleiber, M. 1932. Body size and metabolism. Hilgardia 6:315–353.

Langdon, C. 1993. The significance of respiration in production measurements based on oxygen. Measurement of Primary Production from the Molecular to the Global Scale 197:69–78.

Lewitus, A. J., and T. M. Kana. 1995. Light respiration in six estuarine phytoplankton species: contrasts under photoautotrophic and mixotrophic growth conditions. Journal of Phycology 31:754–761.

Litchman, E., C. A. Klausmeier, O. M. Schofield, and P. G. Falkowski. 2007. The role of functional traits and trade-offs in structuring phytoplankton communities: scaling from cellular to ecosystem level. Ecology Letters 10:1170–1181.

Lopez-Sandoval, D. C., T. Rodriguez-Ramos, P. Cermeno, C. Sobrino, and E. Maranon. 2014. Photosynthesis and respiration in marine phytoplankton: relationship with cell size, taxonomic affiliation, and growth phase. Journal of Experimental Marine Biology and Ecology 457:151–159.

Lopez-Urrutia, A., E. San Martin, R. P. Harris, and X. Irigoien. 2006. Scaling the metabolic balance of the oceans. Proceedings of the National Academy of Sciences of the United States of America 103:8739–8744.

Lynch, M. 1991. Methods for the analysis of comparative data in evolutionary biology. Evolution 45:1065–1080.

Maddison, D. R., K.-S. Schulz, and W. P. Maddison. 2007. The tree of life web project. Zootaxa 1668:19–40.

Maranon, E. 2008. Inter-specific scaling of phytoplankton production and cell size in the field. Journal of Plankton Research 30:157–163.

Maranon, E. 2015. Cell size as a key determinant of phytoplankton metabolism and community structure. Annual Review of Marine Science 7:241–264.

Maranon, E., P. Cermeno, J. Rodrıguez, M. V. Zubkov, and R. P. Harris. 2007. Scaling of phytoplankton photosynthesis

and cell size in the ocean. Limnology and Oceanography 52:2190–2198.
Maranon, E., P. Cermeno, D. C. Lopez-Sandoval, T. Rodriguez-Ramos, C. Sobrino, M. Huete-Ortega, J. M. Blanco, and J. Rodriguez. 2013. Unimodal size scaling of phytoplankton growth and the size dependence of nutrient uptake and use. Ecology Letters 16:371–379.
Marba, N., C. M. Duarte, and S. Agusti. 2007. Allometric scaling of plant life history. Proceedings of the National Academy of Sciences of the United States of America 104: 15777–15780.
Marín, X. F. I. 2015. ggmcmc: graphical tools for analyzing Markov Chain Monte Carlo simulations from Bayesian inference. Journal of Statistical Software 70:1–20.
McGill, B. J., B. J. Enquist, E. Weiher, and M. Westoby. 2006. Rebuilding community ecology from functional traits. Trends in Ecology and Evolution 21:178–185.
Mei, Z. P., Z. V. Finkel, and A. J. Irwin. 2009. Light and nutrient availability affect the size-scaling of growth in phytoplankton. Journal of Theoretical Biology 259:582–588.
Menden-Deuer, S., and E. J. Lessard. 2000. Carbon to volume relationships for dinoflagellates, diatoms, and other protist plankton. Limnology and Oceanography 45:569–579.
Michonneau, F., J. W. Brown and D. J. Winter. 2016. rotl: an R package to interact with the open tree of life data. Methods in Ecology and Evolution 7:1476–1481.
Moal, J., V. Martin-Jezequel, R. Harris, J.-F. Samain, and S. Poulet. 1987. Interspecific and intraspecific variability of the chemical-composition of marine-phytoplankton. Oceanologica acta 10:339–346.
Nadler, L. E., S. S. Killen, E. C. McClure, P. L. Munday, and M. I. McCormick. 2016. Shoaling reduces metabolic rate in a gregarious coral reef fish species. Journal of Experimental Biology 219:2802–2805.
Nagy, K. A. 2005. Field metabolic rate and body size. Journal of Experimental Biology 208:1621–1625.
Nakov, T., E. C. Theriot, and A. J. Alverson. 2014. Using phylogeny to model cell size evolution in marine and freshwater diatoms. Limnology and Oceanography 59:79–86.
Pagel, M. 1999. Inferring the historical patterns of biological evolution. Nature 401:877–884.
Pawar, S., A. I. Dell, and V. M. Savage. 2012. Dimensionality of consumer search space drives trophic interaction strengths. Nature 486:485–489.
Peter, K. H., and U. Sommer. 2012. Phytoplankton cell size: intra- and interspecific effects of warming and grazing. PLoS ONE 7:e49632.
Peters, R. H.. 1986. The ecological implications of body size. Cambridge University Press, New York, New York, USA.
Peters, R. H., and K. Wassenberg. 1983. The effect of body size on animal abundance. Oecologia 60:89–96.
Peterson, B. G., and P. Carl. 2014. PerformanceAnalytics: Econometric tools for performance and risk analysis. R package version 1.4.3541.
Pinheiro, J., D. Bates, S. DebRoy, D. Sarkar, and R Core Team. 2016. nlme: Linear and Nonlinear Mixed Effects Models. R package version 3.1-128, http://cran.r-project.org/package=nlme.
Platt, T., C. L. Gallegos, and W. G. Harrison. 1980. Photoinhibition of photosynthesis in natural assemblages of marine-phytoplankton. Journal of Marine Research 38:687–701.
Plummer, M., N. Best, K. Cowles, and K. Vines. 2006. CODA: convergence diagnosis and output analysis for MCMC. R News 6:7–11.
R Core Team. 2016. A language and environment for statistical computing. R Foundation for Statistical Computing. Vienna, Austria. https://www.r-project.org/.
Rall, B. C., U. Brose, M. Hartvig, G. Kalinkat, F. Schwarzmuller, O. Vucic-Pestic, and O. L. Petchey. 2012. Universal temperature and body-mass scaling of feeding rates. Philosophical Transactions of the Royal Society London. Series B: Biological Sciences 367:2923–2934.
Regaudie-de-Gioux, A., S. Lasternas, S. Agustí, and C. M. Duarte. 2014. Comparing marine primary production estimates through different methods and development of conversion equations. Frontiers in Marine Science 1:1–14.
Savage, V. M., J. F. Gilloly, J. H. Brown, and E. L. Charnov. 2004. Effects of body size and temperature on population growth. American Naturalist 163:429–441.
Schindelin, J., et al. 2012. Fiji: an open-source platform for biological-image analysis. Nature Methods 9:676–682.
Schwaderer, A. S., K. Yoshiyama, P. T. Pinto, N. G. Swenson, C. A. Klausmeier, and E. Litchman. 2011. Eco-evolutionary differences in light utilization traits and distributions of freshwater phytoplankton. Limnology and Oceanography 56:589–598.
Stinchcombe, J. R., Function-valued Traits Working Group, and M., Kirkpatrick. 2012. Genetics and evolution of function-valued traits: understanding environmentally responsive phenotypes. Trends in Ecology & Evolution 27:637–647.
Sun, J., and D. Y. Liu. 2003. Geometric models for calculating cell biovolume and surface area for phytoplankton. Journal of Plankton Research 25:1331–1346.
Taguchi, S. 1976. Relationship between photosynthesis and cell size of marine diatoms. Journal of Phycology 12:185–189.
Thomas, M. K., C. T. Kremer, C. A. Klausmeier, and E. Litchman. 2012. A global pattern of thermal adaptation in marine phytoplankton. Science 338:1085–1088.
Violle, C., M. L. Navas, D. Vile, E. Kazakou, C. Fortunel, I. Hummel, and E. Garnier. 2007. Let the concept of trait be functional!. Oikos 116:882–892.
Warkentin, M., H. M. Freese, U. Karsten, and R. Schumann. 2007. New and fast method to quantify respiration rates of bacterial and plankton communities in freshwater ecosystems by using optical oxygen sensor spots. Applied and Environment Microbiology 73:6722–6729.
West, G. B., J. H. Brown, and B. J. Enquist. 1997. A general model for the origin of allometric scaling laws in biology. Science 276:122–126.
West, G. B., J. H. Brown, and B. J. Enquist. 1999. A general model for the structure and allometry of plant vascular systems. Nature 400:664–667.
West, G. B., J. H. Brown, and B. J. Enquist. 2001. A general model for ontogenetic growth. Nature 413:628–631.
White, C. R., M. R. Kearney, P. G. Matthews, S. A. Kooijman, and D. J. Marshall. 2011. A manipulative test of competing theories for metabolic scaling. American Naturalist 178:746–754.
Wickham, H. 2009. ggplot2: Elegant Graphics for Data Analysis. Springer-Verlag, New York, New York, USA.
Williams, P. J. L. B., and L. M. L. Laurens. 2010. Microalgae as biodiesel & biomass feedstocks: review & analysis of the biochemistry, energetics & economics. Energy & Environmental Science 3:554–590.

Supporting Information

Additional supporting information may be found in the online version of this article at http://onlinelibrary.wiley.com/doi/10.1002/ecy.2032/suppinfo